Investigation of NTM dynamics and control in JT-60SA hybrid scenario

L.Bonalumi[1], E.Alessi[1], L.Figini[1], S.Gabriellini[2], L.Garzotti[2], E.Lazzaro [1], S.Nowak[1], C.Sozzi[1]

[1] *Institute for Science and Technology of Plasma (ISTP),Milan, Italy*

[2] *United Kingdom Atomic Energy Authority, Culham Campus, Abingdon, Oxon OX14 3DB, United Kingdom*

Introduction

Neoclassical tearing modes (NTMs) are resistive instabilities at rational surfaces that grow as magnetic islands and can degrade plasma confinement, leading to disruption. Their nonlinear drive originates from the loss of bootstrap current within the island and scales with the poloidal β, making them particularly impactful in high-β plasmas such as the one expected in JT-60SA (max $B_T/I_p = 2.25T/5.5MA$, major and minor radii $R = 2.92$ m and $a = 1.14$ m.). NTMs can be controlled by injecting electron cyclotron (ECRF) waves inside the magnetic island, through current drive (ECCD) or local heating (ECRH). Experiments dedicated to active NTM control are planned for the third JT-60SA campaign (OP3), but the scenario will be developed and optimized starting from OP2. The evolution of the magnetic island is described through the generalized Rutherford equation (GRE) [1], which governs the time evolution of the island width W. The model computes the evolution of an initial seed island of 2 cm, located in r_s, assuming a linearly stable rational surface ($r_s\Delta'_0 = -2$, with Δ'_0 the linear stability index), accounting for the destabilizing drive of the bootstrap current and the stabilizing effect of the curvature. The stabilizing contributions of the externally driven current and of the associated ohmic heating within the island are also included. In present work, GRE is solved for fixed equilibrium and plasma parameters (stand-alone mode, SA) to perform fast and systematic parameter scans and to study control dynamics that do not substantially modify the background plasma. An alternative configuration is the coupled mode (CM), in which the parameters entering the GRE are updated according to the evolution provided by the integrated transport code JINTRAC [2]. The analysis

Table 1: Heating power and electron density at the resonant surface for the three analyzed scenarios.

Scenario	P_{ECRF} [MW]	P_{PNBI} [MW]	P_{NNBI} [MW]	$n_e(r_s)$ [10^{19} m^{-3}]
Low density (LD)	3	11	5	2.23
Medium density (MD)	3	11	5	3.71
High density (HD)	3	6	10	5.07

is carried out on three JT-60SA OP2 hybrid scenarios ($I_p/B_T = 2.5$ MA$/1.7$ T) taken from [3], characterized by three different density levels and labelled as low (LD), medium (MD) and high density (HD), see Table 1. For each, we evaluate the free 2/1 NTM evolution, the minimum suppression requirements, and control actions to mitigate the risk where the available power is not sufficient for complete stabilization.

Table 2: Summary of the free and controlled 2/1 NTM evolution for the three density scenarios calculating using SA model: maximum island width $W_{\rm sat}$ and saturation time $\tau_{\rm sat}$ (time to reach 90% of $W_{\rm sat}$) from the free evolution, marginal power $P_{\rm req}$ for continuous and modulated injection, and current-drive width $W_{\rm cd}$. Here we set $a_{bs} = 2.6$, $W_d = 2.5$ cm and $\chi_\perp = 0.2$

Scenario	$W_{\rm sat}$ [cm]	$\tau_{\rm sat}$ [s]	$P_{\rm req}$ [MW]	$P_{\rm req}$ [MW] (mod.)	$W_{\rm cd}$ [cm]
Low density	16.64	2.94	2.79	1.42	10.3
Medium density	16.03	1.69	5.07	2.17	12.6
High density	15.00	0.99	9.25	3.40	14.9

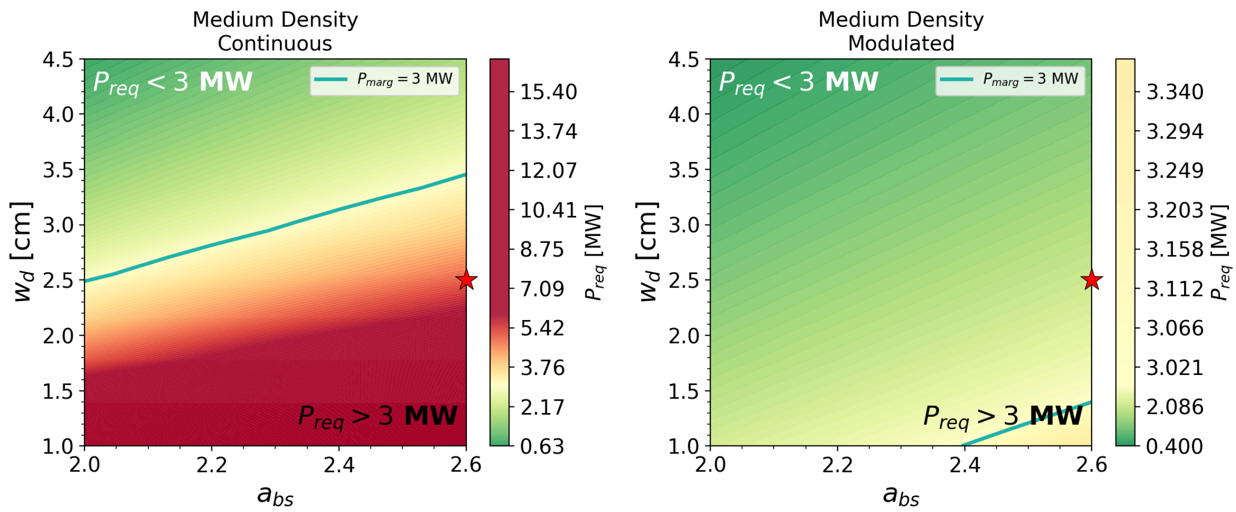

Figure 1: Marginal power $P_{\rm req}$ for 2/1 NTM suppression in the MD scenario versus a_{bs} and W_d for continuous injection (left) and modulated injection (right). The line is the $P_{\rm req} = 3$ MW contour; the star marks the reference point ($a_{bs} = 2.6$, $W_d = 2.5$ cm).

2/1 NTM evolution and stabilization

The island grows and saturates, reaching a maximum width $W_{\rm sat}$ in a timescale set by the saturation time $\tau_{\rm sat}$ (time to reach 90% of $W_{\rm sat}$) (see Table 2). We listed explicitly the value of some parameters whose impact on the evolution is investigated in this work: the coefficient a_{bs} collects the kinetic and geometric factors of the bootstrap drive and is commonly fitted to experiment, with a reference value of 2.6 [4]; the width W_d, at which the bootstrap drive peaks, depends on $(\chi_\perp/\chi_\parallel)|_{W\sim 0}$ and is estimated as 2.5 cm [5, 6]; finally, $\chi_\perp|_{W>>0}$ enters in the heating contribution and sets how well the island retains the heat from the external drive; it can be estimated from data [7] but lacks an established predictive model and values one to two orders of magnitude below the equilibrium diffusivity are commonly used. We adopt $\chi_\perp = 0.2$, which corresponds to around $0.1\,\chi_{{\rm heat},eq}$. A comparison between SA and CM models shows a discrepancy between 2% and 4.5% on the value of the saturation width, making the two models consistent. Using the SA model, the 2/1 NTM dynamics is analyzed under stationary conditions. The LD scenario saturates at the largest width but over the longest time, while increasing density reduces both $W_{\rm sat}$ and $\tau_{\rm sat}$.

The control phase is then assessed by injecting ECRF power at the island O-point.

The controllability of the scenario is expressed in terms of the power requirements P_{req}, defined as:

$$P_{\text{req}} = \min\{P_{ECRF} : dW/dt \leq 0 \,\forall\, W \geq 0\}$$

P_{req} increases with density so that the available 3 MW are sufficient to stabilize the 2/1 mode only in the LD scenario. The application of power with a 50% in-phase duty cycle lowers P_{req} as shown in Table 2, bringing the MD case within the controllable region (see Fig. 1(right)). Several of the parameters entering the model are tied to local plasma quantities at the resonant surface and are difficult to estimate a priori. The impact of the parameter uncertainty is assessed through a scan over $a_{bs} \in [2, 2.6]$ to modulate the strength of the boostrap current and $W_d \in [1, 4.5]$ cm is scanned, following the literature [8]. Their impact on the control requirements is assessed through a scan over the bootstrap coefficient a_{bs} and the saturation width W_d. Figure 1 shows the parametric study of P_{req} for MD across the explored (a_{bs}, W_d) plane. In this work we adopted conservative values for (a_{bs}, W_d) as shown in Figure 1 in the MD case. With these values, available $P_{ECRF} = 3MW$ is not sufficient in the continuous case (left) but allows 2/1 supression if modulating (right). The operating point adopted in this work lies close to the 3 MW boundary, on the side where the available power is not sufficient. A modulated injection leads to a significative enhancement of the controllability.

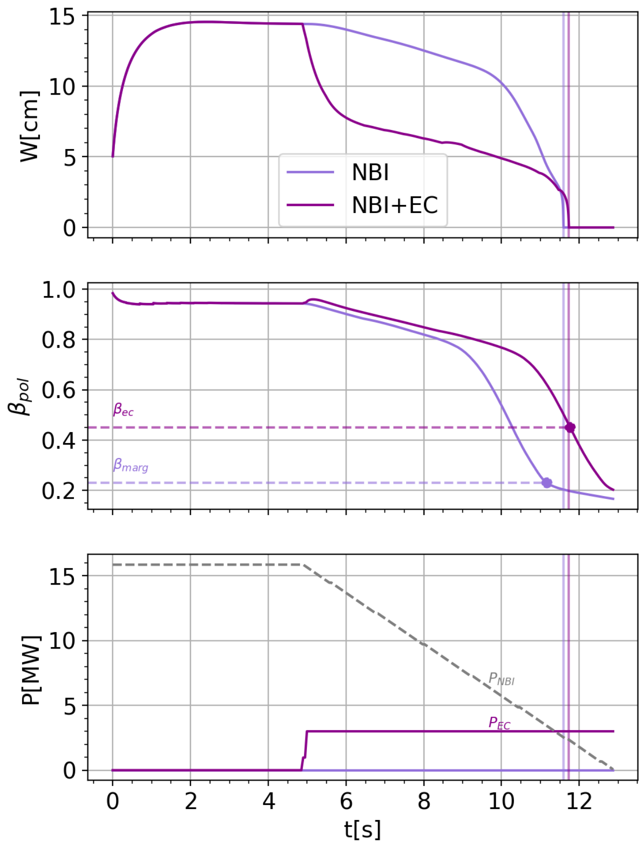

Figure 2: Integrated JETTO–JINTRAC simulation of 2/1 NTM suppression in the high-density scenario, comparing an NBI power ramp-down alone (light) with the same ramp-down assisted by constant 3 MW ECRF injection (dark). Top: island width W; middle: poloidal β, with the marginal value β_{marg} and the ECRF-assisted suppression value β_{EC} indicated (dashed); bottom: NBI and ECRF power. Markers and vertical lines denote the suppression time in each case.

Study for 2/1 control in HD scenario

The HD scenario cannot be stabilized with the available power, even with modulation. The 2/1 mode can in principle self-heal if $\beta_p \leq \beta_{\text{marg}} = 0.2$. In the following, we address the study of a strategy to sustain the ECRF injection with suitable reduction of NBI power. Too large NBI reduction can strongly degrades the discharge performance also with the drawback of changing the linear stability (not considered in the present study). In Figure 2, a linear ramp-down of the NBI power (without ECRF injection) is firstly studied and then compared with the case of continuous

ECRF injection at the island O-point. As evaluated from solving the GRE, complete suppression can be achieved at a higher value $\beta_{\mathrm{EC}} = 0.45 > \beta_{\mathrm{marg}}$, when using ECRF. However, the β_{EC} is yet small and would require a strong NBI reduction of more than 8MW. A further improvement can be obtained with modulated ECRF injection: that raises the suppression threshold to $\beta_{\mathrm{EC,mod}} = 0.82$.

Conclusions

The dynamics and controllability of the 2/1 NTM ($r_s\Delta_0' = -2$, linearly stable regime) have been studied in JT-60SA OP2 hybrid scenarios also taking into account the uncertainty of some parameters on the GRE (Table 2, SA model), focusing on a conservative set of parameters. In the free evolution, the low-density scenario reaches the largest saturated width ($W/a \sim 15\%$), but in a longer time. This scenario is, however, the most controllable: working at lower density and higher temperature increases the current-drive efficiency ($\sim T_e/n_e$), and a continuous 3 MW ECRF injection is sufficient for complete suppression of the 2/1 mode only in this case. For the medium-density scenarios full power modulation is required over the whole expected range of GRE parameters (see Fig. 1). Indeed, the high-density scenario remains critical; integrated JINTRAC simulations were performed to study a possible strategy involving both ECRF injection and partial reduction of the NBI power indicating that ECRF modulation is likely required to not drastically reduce NBI (and hence performance) during the control phase. More defined strategies to control 2/1 NTMs, while keeping high performance, will be developed in view of OP3 campaign, also considering experimental results from OP2.

Acknowledgements

JT-60SA was jointly constructed and is jointly funded and exploited under the Broader Approach Agreement between Japan and EURATOM. This work has been carried out within the framework of the EUROfusion Consortium, funded by the European Union via the Euratom Research and Training Programme (Grant Agreement No 101052200 — EUROfusion). Views and opinions expressed are however those of the author(s) only and do not necessarily reflect those of the European Union or the European Commission. Neither the European Union nor the European Commission can be held responsible for them.

References

[1] V. Basiuk et al., "Simulations of neoclassical tearing mode stabilization in tokamaks," Plasma Phys. Control. Fusion 59, 125012 (2017); https://doi.org/10.1088/1361-6587/aa8c8c

[2] M. Romanelli, et al., "JINTRAC: A system of codes for integrated simulation of tokamak scenarios," Plasma Fusion Res. 9, 3403023 (2014); https://doi.org/10.1585/pfr.9.3403023

[3] S. Gabriellini et al., "Predictive integrated modelling of the hybrid and baseline scenarios of JT-60SA in view of the second operational phase," Nucl. Fusion 65, 056041 (2025); https://doi.org/10.1088/1741-4326/adcb4f

[4] O. Sauter, "Beta limits in long-pulse tokamak discharges," Phys. Plasmas 4, 1654–1664 (1997); https://doi.org/10.1063/1.872270

[5] A. Flaws, The Role of MHD Instabilities in the Improved H-Mode Scenario, Dissertation, Universität Stuttgart, Institut für Plasmaforschung (2009).

[6] R. Fitzpatrick, "Helical temperature perturbations associated with tearing modes in tokamak plasmas," Phys. Plasmas 2, 825–838 (1995); https://doi.org/10.1063/1.871434

[7] L. Bardóczi, et al., "Non-perturbative measurement of cross-field thermal diffusivity reduction at the O-point of 2/1 neoclassical tearing mode islands in the DIII-D tokamak," Phys. Plasmas 23, 052507 (2016); https://doi.org/10.1063/1.4948560

[8] K. Nagasaki et al., "Stabilization of neoclassical tearing mode by ECCD and its evolution simulation on JT-60U tokamak," Nucl. Fusion 45, 1608–1617 (2005); https://doi.org/10.1088/0029-5515/45/12/016